Marshmallow-like macroporous silicone monoliths as reflective standards and high solar-reflective materials

*Gen Hayase**

Research Center for Materials Nanoarchitectonics, National Institute for Materials Science, 1-1 Namiki, Tsukuba, Ibaraki 305-0044, Japan

KEYWORDS. sol-gel, macroporous monoliths, silicone, thermal management, reflective materials

ABSTRACT. The growing need to expand outdoor remote sensing using drones and robots and to mitigate the urban heat island effect has led to an increasing demand for highly reflective materials suitable for outdoor use. I have successfully developed flexible macroporous silicone monoliths that exhibit high diffuse reflectance due to Mie scattering caused by the skeletal structure. The porous silicone materials were prepared by a two-step acetic acid-triethanolamine catalyzed surfactant-free sol-gel process using tetra-, tri-, and difunctional silicon alkoxides as co-precursors. In the optimal sample, the material exhibited a total reflectance of more than 97.5 % in the 400-1100 nm wavelength. This range corresponds to the light detection range of silicon diodes. The optical property suggests potential applications for the silicone monoliths as simple optical calibration targets (reflective standard), providing a viable alternative to conventional materials

such as porous polytetrafluoroethylene or barium sulfate. In addition, high reflectance of the material surfaces across the solar spectrum results in a significant reduction in surface temperature rise when exposed to direct sunlight. With its combination of reflectivity, water repellency, UV resistance, low thermal conductivity, and mid-infrared radiation properties, the macroporous silicone monolith offers promising potential for outdoor thermal management applications.

1. Introduction

In the spectroscopic measurements and colorimetry of material surfaces, materials with known reflectance are indispensable as calibration standards for quantitative optical measurements. Correct calibration of measuring instruments using standard materials provides accurate and reproducible results in the comparative evaluation of optical properties and color, as well as in the normalization of data. Typical materials used as reflective standards include porous barium sulfate and polytetrafluoroethylene (PTFE).[1–3] Driven by technological advancements, the need for labor-saving solutions, and the ability to safely conduct measurements in hazardous areas, there has been a significant increase in the use of drones and robots for remote measurements in recent years.[4] In the automatic image data acquisition using RGB and hyperspectral cameras, it is important to maintain exposure and white balance, and there is a growing demand for reflective target materials to obtain calibration image data. The white target plates that are used in outdoor fields must be weather resistant and have large areas.[5] High weather resistance ensures that the material will not degrade over time, maintaining the reliability of measurement results and reducing the cost of administration. Since telemetry using drones typically involves measuring at high elevations and over large areas, the use of large-area white plates allows for efficient measurements and more accurate data collection. However, existing reflectors require advanced

manufacturing techniques, and high-precision standard materials for outdoor use are generally expensive. Compared to powder sintering and powder coating, which are commonly employed for fabricating highly reflective porous structures, the sol-gel method offers a straightforward and efficient approach to creating porous materials.[6,7] This technique enables precise control of uniformity at the molecular level and fine structure adjustments. Additionally, the sol-gel process can be completed at low temperatures, thereby eliminating the requirement for specialized equipment. Furthermore, the versatility of this method allows for the fabrication of certain materials directly at the measurement site.

Recently, we found the potential of macroporous silicon monoliths prepared by a sol-gel process with time evolution of phase separation as simple highly reflective materials. Our group has studied flexible white silicone monoliths, which we call marshmallow-like gels (MGs), from the copolymerization of tetra-, tri- and difunctional organosilicon alkoxides in aqueous systems.[8,9] Owing to their high porosity, low bulk density, excellent thermal insulation properties, outstanding water repellency, and chemical resistance, these highly flexible and porous materials have been successfully applied in various fields. Consequently, we have reported their utilization in diverse applications, such as thermal insulators,[10] separation media,[9,11] liquid-repellent materials,[12,13] liquid nitrogen retention materials,[10] and giant vesicle formation tools.[11,14,15] In recent applied research, our group has developed an optical tactile sensor that utilizes the intensity change of multiple Mie scattering by a skeleton with a few micrometers in diameter inside the MGs.[16] The silicone framework of MG effectively scatters a wide range of wavelengths in the visible and near-infrared spectrum due to its size. Despite the use of a highly porous silicone material (the porosity is usually above 90 %) as the optical component, the sensor can be made as thin as 1 mm owing to its low external light penetration.

We have already reported that the reason for this property is the high reflectivity of the MG surface. However, the details had not yet been investigated. Silicone materials have been industrialized as a highly reflective material for surface coatings and LEDs,[17] and MGs with viscoelastic phase-separation structures[18] have the potential for similar applications because of their propensity for effective light scattering. Unlike particle aggregates or their composites, MG is a bulk material with the advantages of a large homogeneous area and the ability to be processed into arbitrary shapes. These properties are considered advantageous for the fabrication of easy-to-handle reflective materials. To fabricate MGs specializing in optical properties, a surfactant-free fabrication method with a stable surface morphology was developed, and the relationship between the starting composition and the reflective properties was investigated. In addition, their applicability as high solar-reflective materials for outdoor thermal management is discussed, as this has recently attracted attention owing to environmental concerns.[19–21] Thermal management materials with high solar reflectance tend to require more complex processes in return for their performance. Achieving high reflectance often requires precise control of the material's composition, structure, and properties, which may require multiple steps, specialized equipment for uniform deposition and coating, or advanced techniques. I demonstrate the potential of MG as a bulk optical material that can be reproducibly fabricated by a simple sol-gel process.

This study will demonstrate the potential of MG, synthesized by an optimized sol-gel process, to be deployed extensively as a light-reflective material. Various physical properties of this silicone material as an alternative to existing outdoor reflective materials will be analyzed and discussed.

2. Experimental

Materials. Tetramethoxysilane (TMOS; $Si(OCH_3)_4$), methyltrimethoxysilane (MTMS; $CH3Si(OCH_3)_3$), dimethyldimethoxysilane (DMDMS; $(CH_3)_2Si(OCH_3)_2$), and triethanolamine (TMA) were purchased from Tokyo Chemical Industry Co., Ltd. (Japan). Acetic acid, methanol, and 2-propanol were purchased from Kanto Chemical Co., Inc. (Japan). All the reagents were used as received.

Sample preparation. TMOS (10 mL), MTMS (25 mL), and DMDMS (15 mL) were added to *x* mL ($90 \leq x \leq 210$) of a 5 mM aqueous acetic acid solution. The mixture was stirred for 10 min to hydrolyze the silicon alkoxides. A 1 M TMA aqueous solution ($0.020 \cdot x$ mL) was added to the resulting sol. The mixture was stirred for 3 min and then rapidly transferred to a sealed mold and placed in an 80 °C oven for 12 h. The resulting wet gels were solvent exchanged with methanol followed by 2-propanol and subjected to evaporative drying. The resulting xerogel was designated as MG*x*. The samples were machined on a CNC milling machine (Kitmill CL200, ORIGINALMIND Inc., Japan) as required.

Characterization. The bulk density was calculated within 5 % error on the basis of the weight and volume. Porosity was calculated using the true density obtained via helium pycnometry. Scanning electron microscopy (SEM; TM3000, Hitachi High-Tech Corp., Japan) was used for microstructural observations. The total reflectance was measured using a V-770 ultraviolet–visible–near-infrared (UV–Vis–NIR) spectrometer with an integrating sphere ISN-923 (JASCO Corp., Japan). The reflectance was corrected from the relative reflectance using the diffuse reflectance standard (Spectralon SRS-99-010, Labsphere, Inc., USA) with the calibration certificate of the National Institute of Standards and Technology (NIST, USA) as the reference material. Note that this diffuse reflectance standard is not a strict reference because the data

obtained using ISN-923 includes a specular reflectance component. However, it was used in the calculation for convenience, as no significant errors occurred. An outdoor solar radiation test was conducted on October 29, 2022, on the lawn of the National Institute for Materials Science (140.13310 °E longitude, 36.06948 °N latitude). An MG180 sample with dimensions of 110 mm × 110 mm × 10 mm, half of which was covered with aluminum foil (the surface roughness data obtained using a laser microscope (VK9-9700G, KEYENCE Corp., Japan) is available in Supporting Information), was placed on a perforated stainless-steel plate ~25 cm above the ground. K-type thermocouples were fixed to the surface using Kapton (polyimide) tape. The weather was clear, and the sunshine duration was 100 % during the measurements. Neighborhood weather information was obtained from the Automated Meteorological Data Acquisition System (AMeDAS) on the day of the measurement. This information is provided in Supporting information, and it can be found on the Japan Meteorological Agency website. The temperature was allowed to stabilize for 1 h in a well-ventilated shade. Thereafter, the sample panel was exposed to sunlight at the beginning of the measurement. K-type thermocouples were used to measure the sample surface temperature, and a data logger (AD-5695DL A&D Co., Ltd., Japan) was used to measure the ambient air temperature. Thermal conductivity was measured using a heat flow meter (HFM; HFM 446 Lambda Small, Netzsch GmbH, Germany) using a panel with a size of approximately 110 mm × 110 mm × 10 mm. The temperature difference between the upper and lower hot plates was set as 10 °C, and measurements were obtained at an average temperature of 15–60 °C. The measurement error for each sample was around 3 %. Fourier transform infrared (FTIR) spectra were recorded using IRSpirit-L (Shimadzu Corp., Japan) equipped with an attenuated total reflection (ATR) attachment (QATR-S, Shimadzu Corp., Japan). A total of 100 scans of the sample were recorded at a resolution of 4 cm^{-1}. For spectral emissivity measurements,

an FTIR spectrophotometer (IRTracer-100, Shimadzu Corp., Japan) equipped with a 10 cm inner diameter gold integrating sphere and a liquid nitrogen cooled sensor attachment (GoldenEye III, Systems Engineering Inc., Japan) was used. A total of 200 scans were recorded at a resolution of 8 cm^{-1} to measure relative reflectance/absorbance against the diffuse reflectance standard (Infragold IRT-94-020, Labsphere, Inc., USA). Based on Kirchhoff's law, the obtained IR absorption rate was used as the emissivity. Uniaxial compression tests were performed using a universal tensile testing machine (EZ-SX, Shimadzu Corp., Japan) and a 500 N pressure gauge. The samples were cut into rectangular pieces with dimensions of 15 mm × 15 mm × 8 mm and used for the measurements. Young's modulus was calculated from the change in stress at a compressive strain of 2.5–5.0 %. Water droplet contact angle measurements were made using a custom device with an industrial camera equipped with a telecentric lens and a diffuse LED light source. Images were acquired at 5 different points using 8 μL water droplets and analyzed using ImageJ2 and the Contact Angle plug-in.[22] To confirm UV resistance of MGs, a metal halide lamp (Handy UV 1200mW, Marionetwork Ltd., Japan) was used for testing. The samples were placed on an aluminum plate with a heat sink attached and irradiated with light at an intensity of 300 mW cm^{-2} for a total of 10 h under air cooling, followed by FTIR measurements and mechanical tests to confirm that there were no significant changes before and after irradiation.

3. Results and Discussion

3.1 Process optimization and optical characterization of reflective materials

It is essential to eliminate the inhomogeneity caused by the presence of bubbles in the fabrication of highly reflective monolithic porous materials. First, I improved the sol-gel process to prevent air bubbles from remaining in the monolith. In a previous report, urea was used as a base generator

in an acid–base two-step sol–gel reaction to prepare MGs.[23] Urea provided the advantage that it gradually decomposes and releases ammonia through hydrolysis, resulting in a homogeneous increase in pH throughout the sol and a high yield. However, carbon dioxide, a by-product of hydrolysis, tends to remain in the gel as bubbles. The continuous application of gentle vibration to the sol or pressure using an airtight seal effectively prevented the inclusion of bubbles. Nevertheless, bubbles could not be eliminated in large-volume synthesis. When dilute ammonia water was added to the reaction sol instead of urea, the gel was prone to inhomogenization due to abrupt pH changes, and the skeleton (solid phase) tended to freeze without fully developing the phase-separated structure (Figure S1, Supporting information). As a result, the yield was greatly reduced. However, it was found experimentally that the addition of a weaker base facilitated the formation of a homogeneous gel. Monolithic gels were efficiently obtained when TMA (pK_b = 6.20) was used instead of ammonia water (pK_b = 4.75) with a slight difference in reaction (Figure S2, Supporting information). I could obtain MGs by optimizing the TMA concentration even when the composition ratio of the silicone precursors was changed somewhat. However, the conditions were complex. Therefore, I prepared samples with fixed mixing ratios of organic silicone alkoxides in this study.

In general, the physical properties of monolithic porous materials produced using the sol–gel method can be adjusted by altering the amount of solvent used in the starting process. In the MG*x* system, xerogels were stably produced using a variable (*x*) acetic acid solution volume (90–210 mL). Table 1 lists the prepared samples, and Figure 1 shows the SEM images of the samples. The obtained gels were similar to the MGs obtained using the previously reported urea method. The gels were flexible white monoliths consisting of a continuous skeleton with a diameter of approximately 3 μm (Figure S3, Supporting information). When the amount of solvent was

changed, the density and porosity varied, the skeleton diameter varied negligibly. The total reflectance of each sample (approximately 5 mm thick) was measured using an integrating sphere. All gels showed a high reflectance of over 95.0 % in the visible light range (400–800 nm) (Figure 2a). The reflectance of MG90 and MG210 was slightly lower compared to the other samples. Our recent study has indicated that the optical properties of MGs are affected by Mie scattering (multiple scattering) due to the silicone microframework, characterized by a diameter of several micrometers and a refractive index of 1.40.[16] In samples with high bulk density, i.e., dense scattering sources, multiple scattering is more likely to occur, leading to greater light attenuation. Conversely, in samples with low bulk density, i.e., abundant void spaces, light can penetrate more deeply and may be absorbed. Although the differences observed among the samples in this study were minor, it is clear that forming an optimal microstructure is essential for achieving high reflectance. The reflectance of MG120-180, which had an intermediate bulk density, was 97.5 % or higher at all wavelengths in the main detection range of silicon diodes (400–1100 nm). However, due to the appearance of absorption peaks in the near-infrared light above 1100nm, MGs cannot be used for measurements with InGaAs cameras. Due to the inherent properties of silicone, the MGs showed minimal degradation by moisture absorption from long-term storage or high-intensity UV exposure. Moreover, their superhydrophobic nature (the water contact angle is 153±4°, Figure S4, Supporting information) could lead to a self-cleaning effect on the surface. Because of these characteristics, the MGs are suitable for a wide array of optical applications, such as a standard white board for spectroscopic measurements, material for the inner wall of integrating spheres, and targets for visible-light measurements (Figure 2b). Near-infrared and near-UV reflectance also can be used to create simple UV and IR sensor cards with dyes soaked in the porous structure of MGs (Figure S5, Supporting information).

Table 1. Physical properties of MG*x*.

Sample	Density [g cm^{-3}]	Porosity [%]	Reflectance at a wavelength of 550 nm [%]	Thermal conductivity at 20 °C [W m^{-1} K^{-1}]
MG90	0.167	88.1	97.0	0.0355
MG120	0.135	90.4	98.0	0.0348
MG150	0.122	91.3	98.2	0.0341
MG180	0.112	92.0	98.2	0.0318
MG210	0.112	92.0	97.5	0.0356

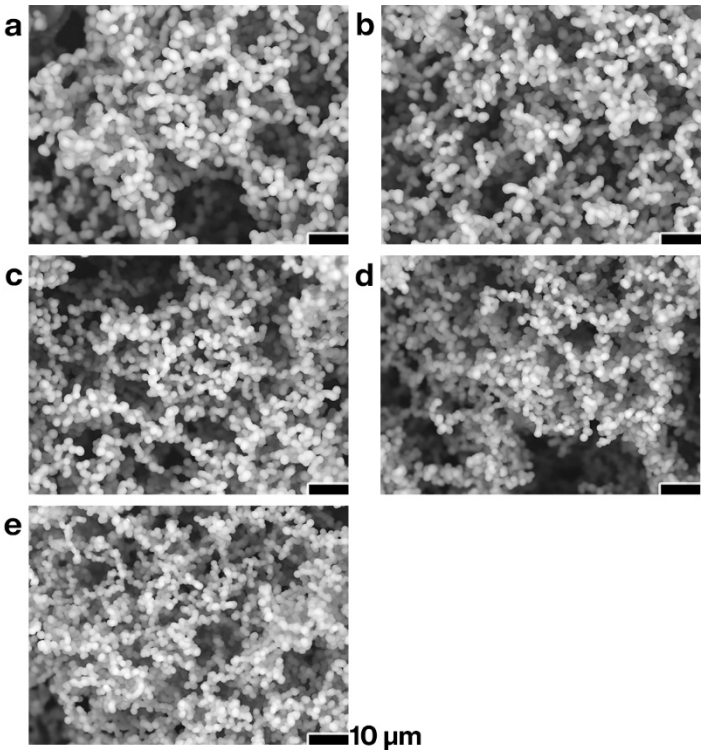

Figure 1. Scanning electron microscope (SEM) images of (a) MG90, (b) MG120, (c) MG150, (d) MG180, and (e) MG210.

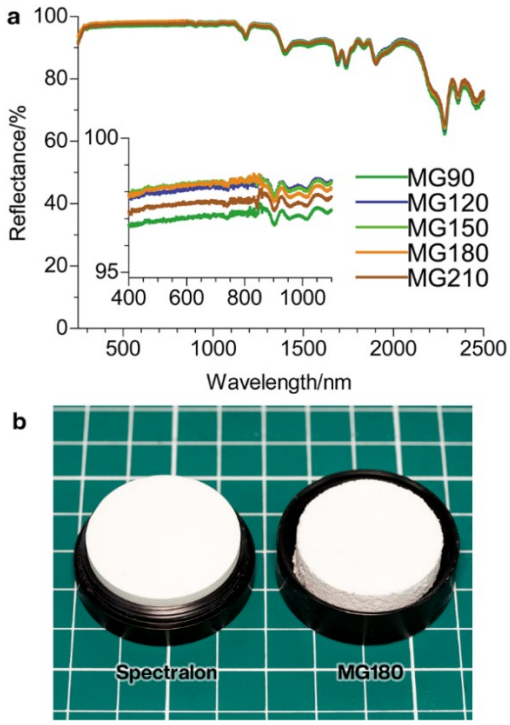

Figure 2. (a) Total light reflectance of MGs. (b) Photograph of Spectralon white reflectance standard and CNC-machined cylindrical MG180. Photograph during the machining is shown in FigureS6, Supporting information.

3.2 Marshmallow-like gel as a high solar-reflective material

Previous studies showed that MGs exhibited low thermal conductivity and that their thermal insulating properties did not decrease with deformation.[23] As silicone is commonly used in practical applications as a solar-reflective paint, it can be used to create a multifunctional thermal management material by adding solar-reflective properties to the thermal insulating properties. Experiments were performed to assess the reflectivity under visible light irradiation using MG180, which displayed high light reflectance the lowest thermal conductivity among all samples due to the balance between bulk density and pore size, factors that influence thermal conductivity in both solid and gas phases.[24]

The total reflectance of MG180 was measured using a spectrophotometer with an integrating sphere at wavelengths of 250–2500 nm (radiation wavelength range of sunlight). Glossy aluminum foil was used as the reference sample owing to the ease of availability and reproducibility. Figure 3a shows that the reflectance of MG180 was better than that of aluminum in the near-UV to NIR range. The optical absorption per unit area on the surfaces of both samples was calculated using the reflectance of MG180 and aluminum foil and the spectral emission intensity of Air Mass 1.5 (AM1.5, the solar spectrum on the surface of Japan),[25,26] and the values were significantly different (Figure 3b). This indicated that unlike aluminum, MG180 absorbed negligible sunlight over the entire wavelength range of light that reached the ground. MG180 showed a few absorption peaks in the NIR reflectance measurements. However, there were no significant peaks for sunlight absorption compared with the visible light region, where the reflectance was higher.

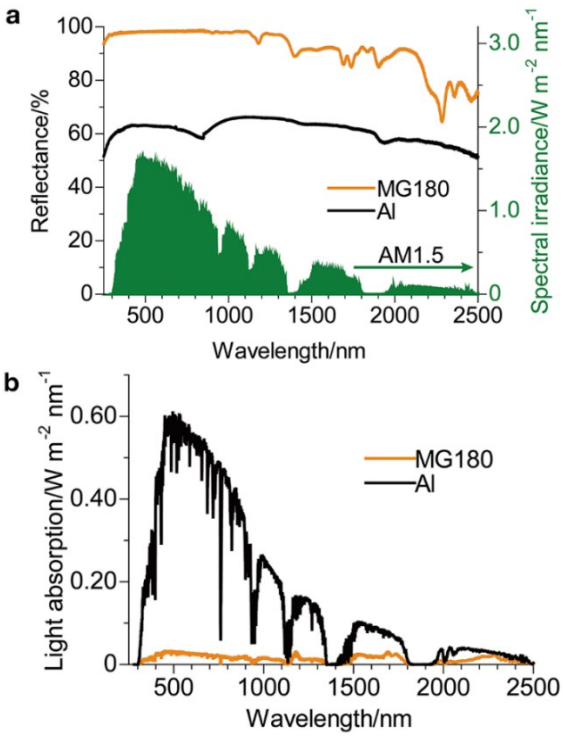

Figure 3. (a) Total light reflectance spectra of MG180 and Al, and AM1.5 (solar radiation).[25,26] (b) Calculated solar absorption spectra of MG180 and Al.

An experiment was conducted by exposing the MG180 to sunny conditions to demonstrate that the increase in surface temperature under solar radiation was significantly suppressed. I prepared MG180 panels of 12 cm × 12 cm × 1 cm dimensions, half of which were sheathed in aluminum foil, with thermocouples positioned in each area. The temperature fluctuations during one hour of daylight exposure in a well-ventilated area are depicted in Figure 4 (refer to the experimental method section for further details on the conditions such as date, time, location, and weather). The aluminum-surfaced part exhibited a rapid temperature surge upon exposure to sunlight, while the temperature of the MG180 panels remained largely unchanged. Utilizing the heat flow meter (HFM) method, I measured the thermal conductivity of MG180, which stood at 33.0 mW m^{-1} K^{-1} at a median temperature of 30 °C, thus indicating superior thermal insulation properties (as shown in Figure 5). These findings suggest that MG180 has potential applicability as a thermal management material for outdoor equipment subjected to direct sunlight, such as external units of air conditioners and cooling pipes.

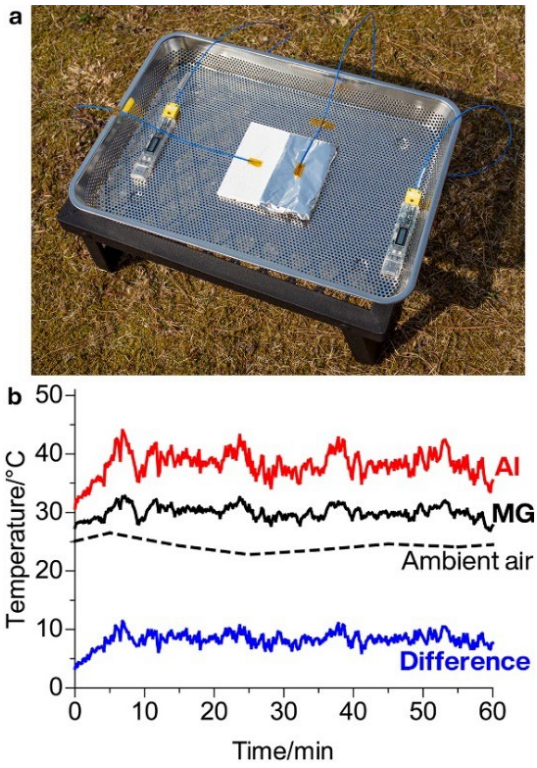

Figure 4. (a) Photograph of MG180/Al sample used for the solar radiation test. (b) Surface temperatures of MG180 and Al under sunlight and ambient air temperature. The blue line shows the temperature difference between Al and MG.

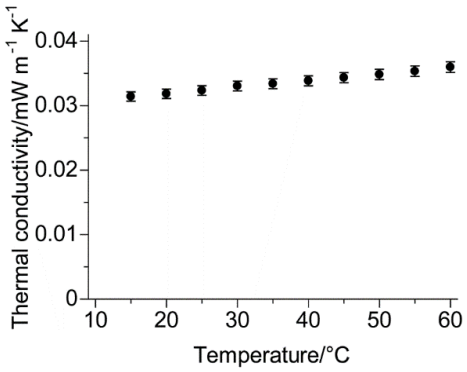

Figure 5. Thermal conductivity of MG180 measured by the HFM method.

Radiative cooling is a material property that is gaining attention in the context of reducing the heat island effect and global warming.[20] Materials that cause efficient radiative cooling have an IR

radiation spectrum in the "atmospheric window" at 8–13 μm.[27] This property has been known for more than 50 years,[28–31] and has been increasingly reported in commodity polymers and silicone-based materials in recent years.[32–37] Diffuse reflectance measurements in the mid-IR region show that MG180 has a high absorption spectrum corresponding to the wavelength of the IR atmospheric window (Figure 6). According to Kirchhoff's law, absorption and emission spectra coincide, [38] suggesting that MG180 thermal management materials could display radiative cooling following solar-heat absorption. Although there have been few reports of heat insulators with passive cooling capabilities,[39] continued improvement of porous silicone materials is expected to lead to further application development. The practicality of macroporous materials, which include but are not limited to current MGs, is limited owing to strength issues such as abrasion resistance. Nevertheless, their performance can be demonstrated in conditions where pressure and force are not applied. The mechanical strength of these materials can be improved by creating composites with other materials. Future development of porous organosiloxane is expected to be used for outdoor applications, taking advantage of its environmental resistance, such as UV resistance and water repellency.

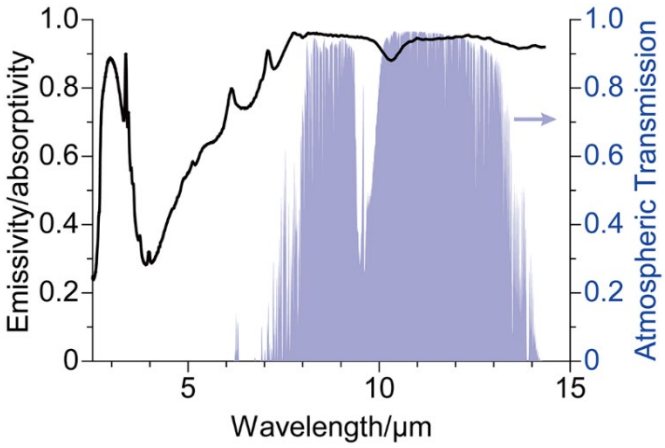

Figure 6. Emission/absorption spectrum of MG180 and the atmospheric window[40] in the mid-IR region.

4. Conclusion

I have successfully synthesized highly reflective porous silicone materials MGs through a surfactant-free copolymerization of organosilicon alkoxides. The fabrication process employs TMA as the base catalyst in a two-step acid-base sol-gel reaction, ensuring bubble-free monolith production. I obtained MGs of various physical properties by modulating the amount of solvent used in the initial composition. Notably, all samples exhibited high total reflectance exceeding 95.0% within the visible light spectrum. The optimized one manifested a reflectance of over 97.5% in the 400-1100 nm wavelength range, which is perceivable by optical devices utilizing silicon photodiodes. This optical property implies its significant potential as a standard reflective target. Furthermore, the sample demonstrated the capability to limit heat absorption effectively by sunlight, thereby suppressing the rise in surface temperature. Exhibiting a low thermal conductivity of approximately 0.032 W m^{-1} K^{-1} near ambient temperature, MG180, akin to all formerly identified silicone materials, possessed radiative cooling properties and efficiently emitted heat within the 8-13 μm atmospheric window. Given their water resistance and UV resilience, these macroporous silicone monoliths offer promising applications for outdoor thermal management.

ASSOCIATED CONTENT

Supporting Information. The following files are available free of charge.

Weather conditions during solar radiation test, surface roughness data of Al foil, SEM image of reference material, FTIR spectra of MG180 and reference material, compressive stress–strain curve of MG180, water repellency of MG180, UV detection using MG impregnated with fluorescent substance, photograph during CNC machining (PDF)

AUTHOR INFORMATION

Corresponding Author

*Email: gen@aerogel.jp

Funding Sources

Any funds used to support the research of the manuscript should be placed here (per journal style).

Notes

The author declares no conflict of interest.

ACKNOWLEDGMENT

I thank Gemini Observatory for providing the atmospheric transmission data. This research was supported by the MEXT Leading Initiative for Excellent Young Researchers (LEADER) program. Research Center for Materials Nanoarchitectonics (MANA) is supported by World Premier International Research Center Initiative (WPI), MEXT, Japan.

REFERENCES

(1) *Diffuse Reflectance Materials, Coatings, Targets, Standards & More*. Labsphere. https://www.labsphere.com/product-category/materials-coatings-targets-standards/ (accessed Oct. 3, 2022).

(2) Weidner, V. R.; Hsia, J. J. Reflection Properties of Pressed Polytetrafluoroethylene Powder. *J. Opt. Soc. Am.* **1981**, *71* (7), 856–861. https://doi.org/10.1364/JOSA.71.000856.

(3) Schutt, J. B.; Arens, J. F.; Shai, C. M.; Stromberg, E. Highly Reflecting Stable White Paint for the Detection of Ultraviolet and Visible Radiations. *Appl. Opt.* **1974**, *13* (10), 2218–2221. https://doi.org/10.1364/AO.13.002218.

(4) Singh, K. D.; Nansen, C. Advanced Calibration to Improve Robustness of Drone-Acquired Hyperspectral Remote Sensing Data. In *2017 6th International Conference on Agro-Geoinformatics*; 2017; pp 1–6. https://doi.org/10.1109/Agro-Geoinformatics.2017.8047061.

(5) Sanches, I. D.; Tuohy, M. P.; Hedley, M. J.; Bretherton, M. R. Large, Durable and Low‐cost Reflectance Standard for Field Remote Sensing Applications. *Int. J. Remote Sens.* **2009**, *30* (9), 2309–2319. https://doi.org/10.1080/01431160802549377.

(6) Jeffrey Brinker, C.; Scherer, G. W. *Sol-Gel Science: The Physics and Chemistry of Sol-Gel Processing*; Academic Press, 1990. pp. 853-857.

(7) Lévy, D.; Zayat, M. *Sol-Gel Handbook: Synthesis, Characterization, and Applications*; Wiley-VCH Verlag GmbH, 2015. pp. 317-344.

(8) Hayase, G.; Kanamori, K.; Nakanishi, K. New Flexible Aerogels and Xerogels Derived from Methyltrimethoxysilane/Dimethyldimethoxysilane Co-Precursors. *J. Mater. Chem.* **2011**, *21* (43), 17077–17079. https://doi.org/10.1039/C1JM13664J.

(9) Hayase, G.; Kanamori, K.; Fukuchi, M.; Kaji, H.; Nakanishi, K. Facile Synthesis of Marshmallow-like Macroporous Gels Usable under Harsh Conditions for the Separation of Oil and Water. *Angew. Chem. Int. Ed.* **2013**, *52* (7), 1986–1989. https://doi.org/10.1002/anie.201207969.

(10) Hayase, G.; Ohya, Y. Marshmallow-like Silicone Gels as Flexible Thermal Insulators and Liquid Nitrogen Retention Materials and Their Application in Containers for Cryopreserved Embryos. *Appl. Mater. Today* **2017**, *9*, 560–565. https://doi.org/10.1016/j.apmt.2017.10.004.

(11) Hayase, G.; Nomura, S.-I. M. Macroporous Silicone Sheets Integrated with Meshes for Various Applications. *ACS Appl. Polym. Mater.* **2019**, *1* (8), 2077–2082. https://doi.org/10.1021/acsapm.9b00382.

(12) Hayase, G.; Kanamori, K.; Hasegawa, G.; Maeno, A.; Kaji, H.; Nakanishi, K. A Superamphiphobic Macroporous Silicone Monolith with Marshmallow-like Flexibility. *Angew. Chem. Int. Ed.* **2013**, *52* (41), 10788–10791. https://doi.org/10.1002/anie.201304169.

(13) Takei, T.; Terazono, K.; Araki, K.; Ozuno, Y.; Hayase, G.; Kanamori, K.; Nakanishi, K.; Yoshida, M. Encapsulation of Hydrophobic Ingredients in Hard Resin Capsules with Ultrahigh Efficiency Using a Superoleophobic Material. *Polym. Bull.* **2016**, *73* (2), 409–417. https://doi.org/10.1007/s00289-015-1497-y.

(14) Hayase, G.; Nomura, S. M. Large-Scale Preparation of Giant Vesicles by Squeezing a Lipid-Coated Marshmallow-like Silicone Gel in a Buffer. *Langmuir* **2018**, *34* (37), 11021–11026. https://doi.org/10.1021/acs.langmuir.8b01801.

(15) Nomura, S. M.; Shimizu, R.; Archer, R. J.; Hayase, G.; Toyota, T.; Mayne, R.; Adamatzky, A. Spontaneous and Driven Growth of Multicellular Lipid Compartments to Millimeter Size from Porous Polymer Structures. *ChemSystemsChem* **2022**, *4* (5), e202200006. https://doi.org/10.1002/syst.202200006.

(16) Hayase, G. Optical Tactile Sensor Using Scattering inside Sol-Gel-Derived Flexible Macroporous Monoliths. *Sens. Actuators A Phys.* **2023**, *354*, 114253. https://doi.org/10.1016/j.sna.2023.114253.

(17) *Optically Reflective Silicone Materials for LED Lighting I DuPont*. https://www.dupont.com/electronic-materials/optically-reflective-silicone-materials.html (accessed Feb. 25, 2023).

(18) Tanaka, H. Viscoelastic Phase Separation. *J. Phys. Condens. Matter* **2000**, *12* (15), R207. https://doi.org/10.1088/0953-8984/12/15/201.

(19) Santamouris, M.; Synnefa, A.; Karlessi, T. Using Advanced Cool Materials in the Urban Built Environment to Mitigate Heat Islands and Improve Thermal Comfort Conditions. *Solar Energy* **2011**, *85* (12), 3085–3102. https://doi.org/10.1016/j.solener.2010.12.023.

(20) Raman, A. P.; Anoma, M. A.; Zhu, L.; Rephaeli, E.; Fan, S. Passive Radiative Cooling below Ambient Air Temperature under Direct Sunlight. *Nature* **2014**, *515* (7528), 540–544. https://doi.org/10.1038/nature13883.

(21) Rosati, A.; Fedel, M.; Rossi, S. NIR Reflective Pigments for Cool Roof Applications: A Comprehensive Review. *J. Clean. Prod.* **2021**, *313*, 127826. https://doi.org/10.1016/j.jclepro.2021.127826.

(22) Rueden, C. T.; Schindelin, J.; Hiner, M. C.; DeZonia, B. E.; Walter, A. E.; Arena, E. T.; Eliceiri, K. W. ImageJ2: ImageJ for the next Generation of Scientific Image Data. *BMC Bioinformatics* **2017, *18*** (1), 529. https://doi.org/10.1186/s12859-017-1934-z.

(23) Hayase, G. Surfactant-Free Aqueous Fabrication of Macroporous Silicone Monoliths for Flexible Thermal Insulation. *Bull. Chem. Soc. Jpn.* **2021**, *94* (9), 2210–2215. https://doi.org/10.1246/bcsj.20210189.

(24) Lu, X.; Caps, R.; Fricke, J.; Alviso, C. T.; Pekala, R. W. Correlation between Structure and Thermal Conductivity of Organic Aerogels. *J. Non-Cryst. Solids* **1995**, *188* (3), 226–234. https://doi.org/10.1016/0022-3093(95)00191-3.

(25) *Reference Air Mass 1.5 Spectra*. https://www.nrel.gov/grid/solar-resource/spectra-am1.5.html (accessed Oct. 03, 2022).

(26) Gueymard, C. A.; Myers, D.; Emery, K. Proposed Reference Irradiance Spectra for Solar Energy Systems Testing. *Sol. Energy* **2002**, *73* (6), 443–467. https://doi.org/10.1016/S0038-092X(03)00005-7.

(27) *The Sites*. Gemini Observatory. https://www.gemini.edu/observing/telescopes-and-sites/sites (accessed Oct. 3, 2022).

(28) Catalanotti, S.; Cuomo, V.; Piro, G.; Ruggi, D.; Silvestrini, V.; Troise, G. The Radiative Cooling of Selective Surfaces. *Sol. Energy* **1975**, *17* (2), 83–89. https://doi.org/10.1016/0038-092X(75)90062-6.

(29) Bartoli, B.; Catalanotti, S.; Coluzzi, B.; Cuomo, V.; Silvestrini, V.; Troise, G. Nocturnal and Diurnal Performances of Selective Radiators. *Appl. Energy* **1977**, *3* (4), 267–286. https://doi.org/10.1016/0306-2619(77)90015-0.

(30) Orel, B.; Gunde, M. K.; Krainer, A. Radiative Cooling Efficiency of White Pigmented Paints. *Sol. Energy* **1993**, *50* (6), 477–482. https://doi.org/10.1016/0038-092X(93)90108-Z.

(31) Farooq, A. S.; Zhang, P.; Gao, Y.; Gulfam, R. Emerging Radiative Materials and Prospective Applications of Radiative Sky Cooling - A Review. *Renew. Sustain. Energy Rev.* **2021**, *144*, 110910. https://doi.org/10.1016/j.rser.2021.110910.

(32) Srinivasan, A.; Czapla, B.; Mayo, J.; Narayanaswamy, A. Infrared Dielectric Function of Polydimethylsiloxane and Selective Emission Behavior. *Appl. Phys. Lett.* **2016**, *109* (6), 061905. https://doi.org/10.1063/1.4961051.

(33) Kou, J.-L.; Jurado, Z.; Chen, Z.; Fan, S.; Minnich, A. J. Daytime Radiative Cooling Using Near-Black Infrared Emitters. *ACS Photonics* **2017**, *4* (3), 626–630. https://doi.org/10.1021/acsphotonics.6b00991.

(34) Alden, J. D.; Atiganyanun, S.; Vanderburg, R.; Lee, S. H.; Plumley, J. B.; Abudayyeh, O. K.; Han, S. M.; Han, S. E. Radiative Cooling by Silicone-Based Coating with Randomly Distributed Microbubble Inclusions. *J. Photonics Energy* **2019**, *9* (3), 032705. https://doi.org/10.1117/1.JPE.9.032705.

(35) Zhou, L.; Song, H.; Liang, J.; Singer, M.; Zhou, M.; Stegenburgs, E.; Zhang, N.; Xu, C.; Ng, T.; Yu, Z.; Ooi, B.; Gan, Q. A Polydimethylsiloxane-Coated Metal Structure for All-Day Radiative Cooling. *Nat. Sustain.* **2019**, *2* (8), 718–724. https://doi.org/10.1038/s41893-019-0348-5.

(36) Zhao, H.; Sun, Q.; Zhou, J.; Deng, X.; Cui, J. Switchable Cavitation in Silicone Coatings for Energy-Saving Cooling and Heating. *Adv. Mater.* **2020**, *32* (29), e2000870. https://doi.org/10.1002/adma.202000870.

(37) Wang, T.; Wu, Y.; Shi, L.; Hu, X.; Chen, M.; Wu, L. A Structural Polymer for Highly Efficient All-Day Passive Radiative Cooling. *Nat. Commun.* **2021**, *12* (1), 365. https://doi.org/10.1038/s41467-020-20646-7.

(38) Granqvist, C. G.; Hjortsberg, A. Radiative Cooling to Low Temperatures: General Considerations and Application to Selectively Emitting SiO Films. *J. Appl. Phys.* **1981**, *52* (6), 4205–4220. https://doi.org/10.1063/1.329270.

(39) Leroy, A.; Bhatia, B.; Kelsall, C. C.; Castillejo-Cuberos, A.; Di Capua H, M.; Zhao, L.; Zhang, L.; Guzman, A. M.; Wang, E. N. High-Performance Subambient Radiative Cooling Enabled by Optically Selective and Thermally Insulating Polyethylene Aerogel. *Sci Adv* **2019**, *5* (10), eaat9480. https://doi.org/10.1126/sciadv.aat9480.

(40) Lord, S. D. *A New Software Tool for Computing Earth's Atmospheric Transmission of Near- and Far-Infrared Radiation*; NASA Ames Research Center, 1992. https://ntrs.nasa.gov/citations/19930010877.

ToC